

NLP optimization of a methanol plant by using multi-parameter optimization

Anita Kovač Kralj*

Department of Chemistry and Chemical Engineering, University of Maribor, Smetanova 17, Maribor, Slovenia

ABSTRACT

This paper describes the application of a nonlinear programming (NLP) mathematical method within an existing process, using simultaneous process and energy system multi-parameter optimization. It presents an expansion of a retrofit design case study using Combined Heat and Power (CHP), with the following new topic as key themes: including degrees of conversion at the catalyst bed-level in the reactor model, using hydrogen separation from purge gas, and energy generation using hydrogen fuel cells. The aim of this article is to connect process optimization with renewable energy generation, using waste hydrogen from the purge gas of the methanol reactor as fuel in the fuel cells. The separation of hydrogen is a continuous process of cleaning waste H_2 , without costly production and storage of the fresh one. Fuel cells and open gas turbine electricity cogeneration can be optimized simultaneously using the NLP algorithm. The NLP model contains equations for parametric optimization, including degrees of conversion at successive catalyst bed-levels. The NLP model is often used to optimize complex and energy intensive continuous processes. This procedure does not guarantee the global cost optimum, but it does lead to good designs, perhaps near-optimum ones. The optimization approach is illustrated using a complex low-pressure Lurgi methanol plant, giving

an additional profit of 2.65 MEUR/a. The plant, which produces methanol, has a surplus of hydrogen (H_2) flow rate in its purge gas. H_2 should be separated from the purge gas by an existing pressure swing adsorption (PSA) column. Pure H_2 can be used as fuel in the hydrogen fuel cells.

KEYWORDS: catalyst, degree of conversion, fuel cell, hydrogen separation, NLP model, simultaneous optimization, methanol

1. INTRODUCTION

NLP can be used for multi-parameter optimization, which includes energy and process systems optimization using mathematical methods of nonlinear programming. The goal of multi-parameter optimization, which includes energy and process systems optimization, is to generate more alternatives and search for the best solution from them. Alternatives using fuel cells and catalysis are included. Horlock [1] has defined the criterion for primary energy savings at combined multi-parameter optimization of Combined Heat and Power (CHP) plants. A comparative study has been performed based on this criterion for different configurations of a CHP plant. Havelsky [2] analysed the multi-parameter problem of energy efficiency evaluation in a system for combined heat, cooling, and power production. A step-wise methodology for gas turbine integration, including multi-parameter optimization of heat and power cogeneration, was developed by Axelsson and co-authors [3].

*anita.kovac@uni-mb.si

The mathematical optimisation method can be classified as a simultaneous approach, which accurately accounts for capital and energy trade-offs. The NLP model [4], based on mathematical programming, can be used for multi-parameter optimization, and process modifications.

Optimization of processes can be carried out using short-cut or extended short-cut models for reactor simulation. In our work to date, we have not been using any extended short-cut methods for the reactors. In this study we wanted to upgrade the reactor models for using catalyst bed level-to-level conversions. Several research studies have been published on catalyst selectivity for methanol production. Moreover, several studies have been reported on the kinetic modelling of methanol synthesis and deactivation models regarding the effects of temperature and gas composition [5].

2. Multi-parameter energy and process systems optimization

The aim of this article is to use the simultaneous optimization approach and to incorporate multi-parameter energy and process systems' optimization into the procedure, in order to obtain a good process design or retrofit. This approach is very useful within an industrial environment. A number of possible alternatives can be included in the optimization model and computer based tools can search for the best new process system or modification for an existing plant. The process system retrofit model used as a case study, involves fuel cells, as well as catalytic reaction, separation, CHP, and a heat exchanger network.

This paper presents the extension of a retrofit design including hydrogen separation for use in fuel cells, and degrees of conversion at each catalyst bed-level in the reactor.

2.1. Fuel-cell

A hydrogen fuel-cell consists of two electrodes. Oxygen passes over one electrode and hydrogen over the other, thus generating electricity, water and heat. Hydrogen fuel is fed to the anode, and oxygen (or air) enters the fuel cell through the cathode. The hydrogen atom splits into a proton and an electron, which take different paths to the

cathode. The proton passes through the electrolyte. The electrons create separate currents that can be utilized before they return to the cathode, in order to be reunited with the hydrogen and oxygen into a water molecule.

Low temperature fuel-cells can operate efficiently when using pure hydrogen; therefore, hydrogen shall be separated from outlet gas by using an adsorption system. The advantages of using purge hydrogen in fuel-cells are:

- higher electro-chemical activity because of lower temperatures
- the by-product, which could poison the fuel-cells, cannot be produced
- operating time can be extended.

In fuel cells, a flow rate of pure H₂, equal to 0.01 mol/s, or 0.02 g/s can produce electric power of 1 kW, and twice the heat flow rate (Φ_{fc}), from an investment of 2 125 EUR/kW, using a solid polymer membrane-type fuel cells [6]. A simplified fuel cell model of one type of fuel cells can be used for the NLP algorithm. The electrical energy can be calculated from the power of fuel cells (P_{fc} , Eq. 2) by using the molar energy (E_{fc} , Eq. 1) in the fuel cell:

$$E_{fc} = P_{fc} E_{fc} = 1 \text{ kW} / (0.01 \text{ mol s}^{-1}) = 100 \text{ kJ mol}^{-1} \quad (1)$$

using the amount flow rate of the pure H₂ component ($F^{\text{out, p, H}_2}$; Eq. 6 in chapter 2.2).

$$P_{fc} = E_{fc} F^{\text{out, p, H}_2} \quad (2)$$

Heat flow rate in fuel-cells (Φ_{fc}) can be calculated by Eq. 3 [6]:

$$\Phi_{fc} = 2P_{fc} \quad (3)$$

The objective function (Eq. 4) of the NLP model is to maximize the annual profit, V ; it includes electricity cogeneration in fuel-cells (P_{fc}), heat flow rate in fuel-cells (Φ_{fc}), annual depreciation of fuel cells (C_{fc}), and cost of hydrogen separation from the purge gas (C_{H_2}):

$$V_{\max} = C_{el} \cdot P_{fc} + C_{\text{heat}} \cdot \Phi_{fc} - C_{fc} \cdot P_{fc} \cdot r - C_{H_2} \cdot F_{H_2} \cdot r \quad (4)$$

The parameter r is the payback multiplier. The maximum additional annual profit is included

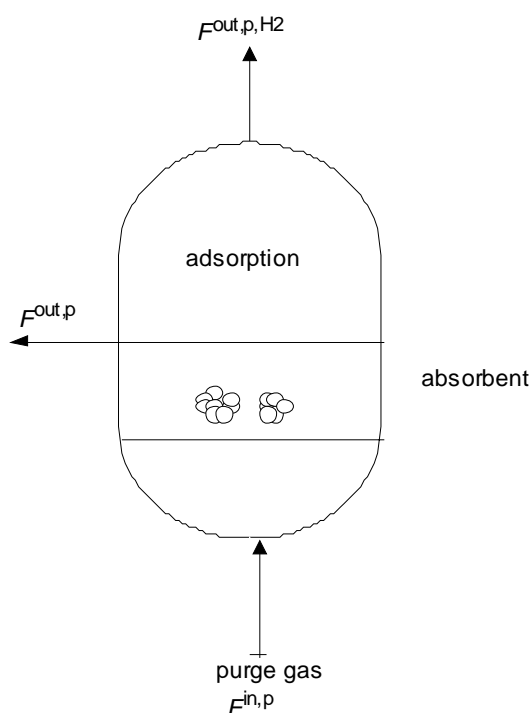


Figure 1. Pressure Swing Adsorption (PSA) column.

within the objective function of the case study, as defined in chapter 3.2.

2.2. H₂ separation

All methanol production plants have a surplus of hydrogen (H₂) flow rate in purge gas. H₂ can be separated from the purge gas by a pressure swing adsorption (PSA) column (Fig. 1) removing N₂, CO, CO₂, CH₄ and H₂O, in order to deliver hydrogen at 90.0–99.9 % purity level. Pure H₂ can be used as fuel in the fuel cells.

The mass balance of the PSA column in the NLP model is simplified:

$$F^{\text{in},p} = F^{\text{out},p,H_2} + F^{\text{out},p} \quad (5)$$

$$F^{\text{out},p,H_2} = F^{H_2} \cdot \eta_{\text{PSA}} \quad (6)$$

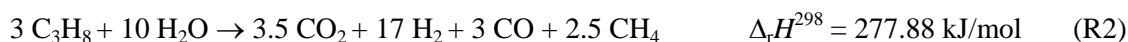
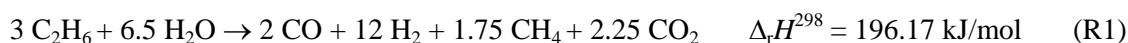
The inlet stream ($F^{\text{in},p}$) is a sum of the outlet streams of the pure H₂ component (F^{out,p,H_2}), and the remaining purge gas ($F^{\text{out},p}$). F^{H_2} is the flow rate of H₂ in the purge gas ($\eta_{\text{PSA}} = 0.6$).

3. Case study

3.1. Original process and retrofit options

The proposed use of catalysis and fuel cell models was applied to an existing complex, low-pressure Lurgi methanol process [7]. Our first goal was to find a good retrofit of the existing production plant (Fig. 2); simultaneous multi-parameter energy and process systems' optimization was used for this purpose. The process system involved only part of the total plant: fuel cells, catalyzed reactions, separation, and heat exchange. The second aim of this work was to use the waste hydrogen from the purge gas as fuel in the fuel cells. Separation of the hydrogen was carried out continuously by cleaning the purge gas, thus avoiding costly production and storage of a fresh one. The third aim was to include the model using degrees of conversion at each catalyst bed-level in the reactor.

A simplified flow-sheet of the methanol process is presented in Figure 3. In the first subsystem, natural gas is desulphurized in D101, and heated-up in a steam reformer REA-1 to 825 °C and 17.5 bar pressure. Synthesis gas (a mixture of CO, CO₂, CH₄ and H₂) is produced from the natural gas and steam at the NiO catalyst:



The hot stream of synthesis gas is cooled in the boiler E107, in heat exchangers (E109–E111), in the air cooler EA101, and in the water cooler E112. The condensate expands in flash separators: F1, F2, F107 and F108. The synthesis gas is compressed in a two-

stage (G201-I and G201-II) compressor. In the second subsystem, methanol is produced by the catalytic hydrogenation of carbon monoxide and/or carbon dioxide in the reactor REA-2, using the following three main reversible reactions ($r = R6, R7, R8$):

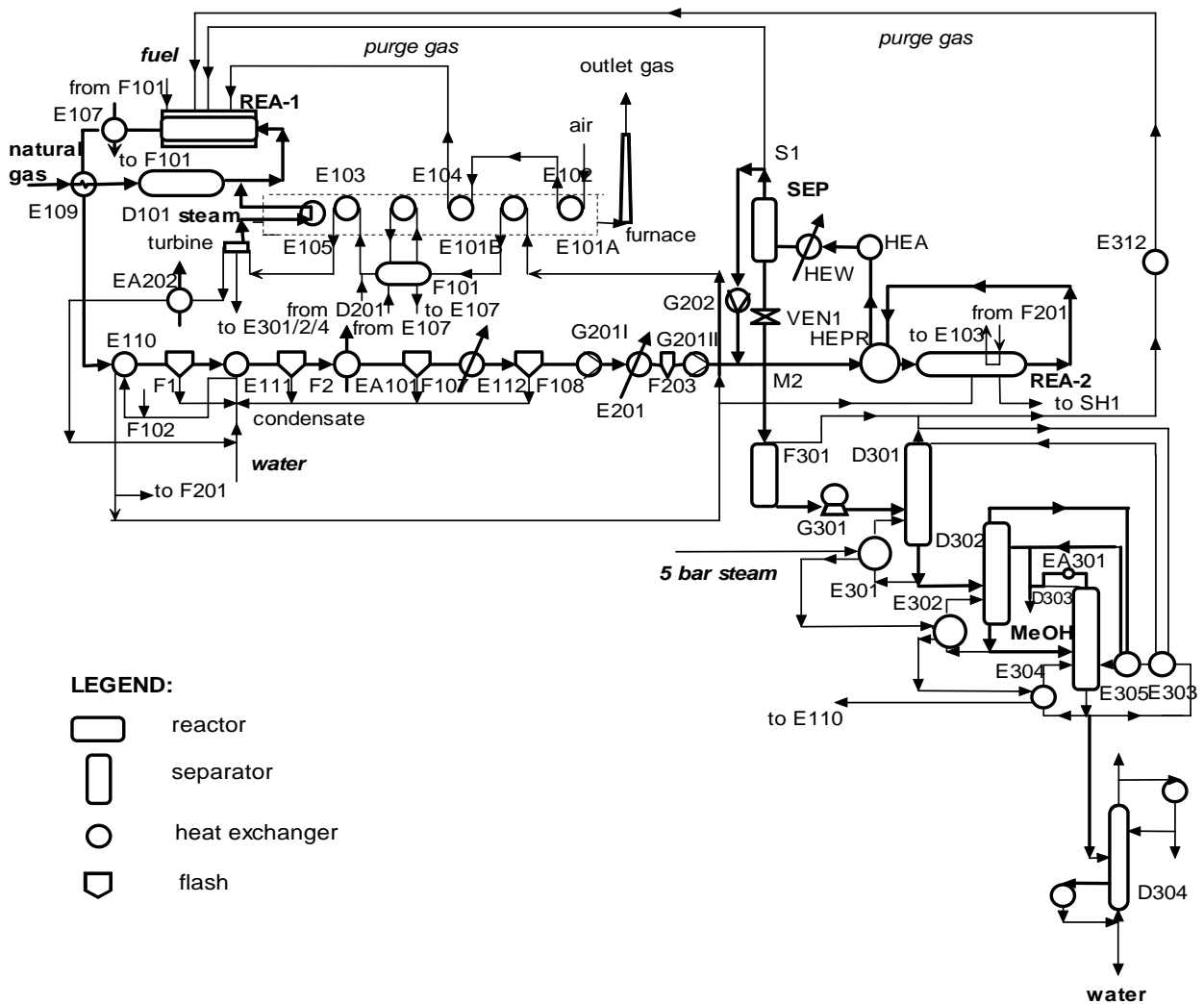
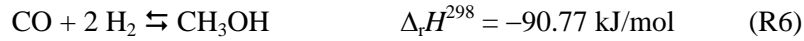


Figure 2. Process flow diagram of a low-pressure Lurgi methanol plant.

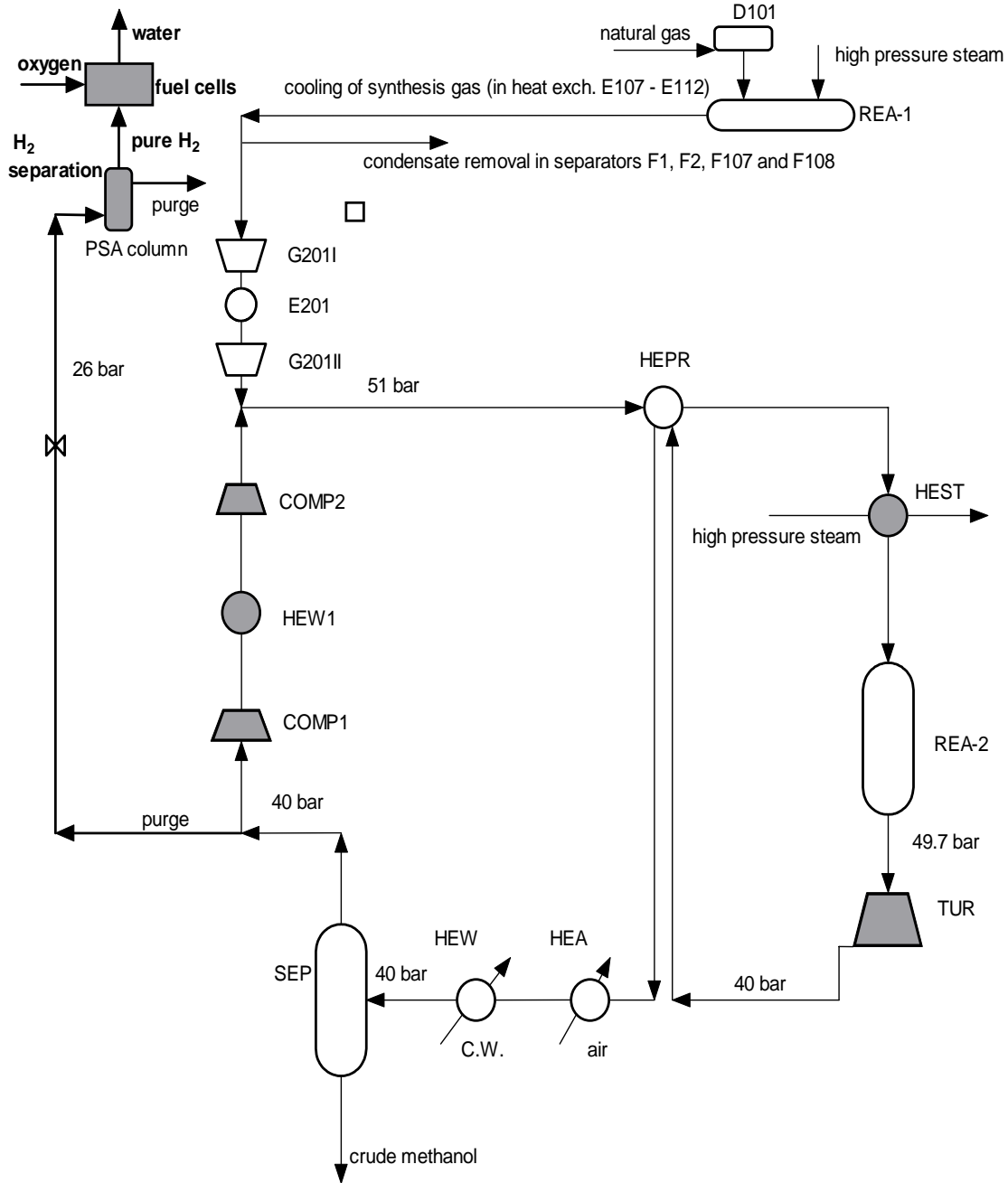


Figure 3. Simplified flow-sheet of a methanol plant with fuel cells.

The second reactor REA-2 is operated under a pressure of 51 bar, and the non-converted gas is recycled. The outlet crude methanol stream of REA-2 is cooled with its inlet stream in the heat exchanger HEPR, in the air cooler HEA, and in the water cooler HEW. The methanol is flashed in the separator, SEP. In the third subsystem

(distillation columns D301–D302 in Fig. 2, not shown in Fig. 3), crude methanol is refined to pure methanol by distillation in the purification section of the process, in order to remove water and a variety of other impurities. The high-pressure reactor REA-2 is operated using the existing parameters, and the non-converted gas is recycled.

The high recycle ratio and operating pressure of the reactor are exploited to produce electricity, using a gas turbine (TUR) placed downstream of the reactor, and REA-2 outlet gas as a working fluid. The reactor inlet stream is heated by a process stream (HEPR) or by high-pressure steam (HEST) or by using a combination of both. The liquid outlet stream of the separator is the product, while the recycled gas stream is compressed to 51 bar in a new, two-stage compressor (COMP1, COMP2) with intermediate water cooling (HEW1). The producer can use the existing, inactive pressure swing adsorption (PSA) column for H₂ separation. The pure H₂ can be used as fuel in the fuel cells.

3.2. The NLP model

The methanol process parameters are optimized using a nonlinear programming (NLP) model. Mixed Integer Nonlinear Programming (MINLP) was not used as we did not have any structural variables, but only continuous ones. The mathematical model includes integration of heat flows, increased production, a realistic catalyst model, combined heat and electricity production (CHP), and fuel cells. Temperatures and molar heat capacities are variable within the limits of the real industrial data. Simultaneous optimization could increase annual profit.

The parameters in the retrofit model of the heat exchanger network, flashes, compressors, mixer, splitters, reactors, and the turbine, were simultaneously optimized using the GAMS/ MINOS software [8]. This NLP can be solved using a large-scale reduced gradient method (e. g. MINOS).

This problem is non-convex, it does not guarantee a global optimization solution, but it quickly gives good results for non-trivial, complex processes. It contains variables of the process parameters: molar heat capacities, material flow rates, heat flow rates, and temperatures, which are limited by real constraints. It has variable heat capacity flow rates for all the streams. This model contains equations for parameter optimization. The NLP model is formulated using a simplified process structure of the Combined Heat and Power, and the additional possibility of electricity production in fuel-cells. The different types of fuel-cells have not been dealt with, so far.

The model of the crude methanol reactor REA-2 considers all the reactions r ($r = 1, \dots, R$) of the synthesis gas, and the crude methanol production, including those equations for the equilibrium constants K_r of reactions r (Equations 7 and 8), and the equilibrium conversions of components s (CO₂, CO, H₂, CH₄, C₂H₆, C₃H₈, C₄H₁₀, H₂O, CH₃OH, CH₃OCH₃, CH₃CH₂CH₂OH; $s = 1, \dots, S$, Eqs. 10–12). The equilibrium constant K_r depends on the temperature (T), Gibbs energy (G) and gas constant (R) (Eqs. 8 and 9):

$$\sum (y_s)^{\nu_s} = p^{\nu} \cdot K_r \quad r = 1, \dots, R \quad (7)$$

where y is equilibrium gas composition, ν is stoichiometric coefficient and p is pressure.

$$K_r = e^{(-\Delta G_r/RT)} \quad (8)$$

Gibbs (free) energy (ΔG) can be calculated by using equation 9:

$$\Delta G_r = J_r - RT(\Delta a_r \ln T + \Delta b_r \cdot T/2 + \Delta c_r \cdot T^2/6 + \Delta d_r/(2T^2) + I_r), \quad r = 1, \dots, R \quad (9)$$

where a_r, b_r, c_r, d_r are heat capacity constants of reaction r and I_r is integration constant of reaction r .

The conversion rate of reaction r (ω_r) can be calculated from a differential change in the extent of reaction ($d\xi_r$), after time t :

$$\omega_r = d\xi_r/dt \quad r = 1, \dots, R \quad (10)$$

The amount flow rate F is defined as:

$$F_s = dn_s/dt \quad s = 1, \dots, S \quad (11)$$

and outlet's amount flow rate for component s is:

$$F_{s, \text{out}} = F_{s, \text{in}} + \sum_r \nu_{s,r} \omega_r \quad s = 1, \dots, S \quad r = 1, \dots, R. \quad (12)$$

This model was extended by additional equations regarding heat balances for the retrofit of heat exchangers, as listed in Eq. 13, using variable heat capacity flow rates (CF_i), and temperatures (T_i) for determining heat flow rate (Φ_i):

$$(T_{i,n}^{\text{in}} - T_{i,n}^{\text{out}}) \cdot CF_{i,n} = \Phi_n$$

$$n = \text{E107, E109, E110, E111, EA101, E112, E201, HEPR, HEA, and HEW} \in \mathbf{N} \quad (13)$$

$$\Delta_{\ln} T_n = (T_{i,n}^{\text{in}} - T_{j,n}^{\text{out}}) - (T_{i,n}^{\text{out}} - T_{j,n}^{\text{in}}) / \ln(T_{i,n}^{\text{in}} - T_{j,n}^{\text{out}}) / [(T_{i,n}^{\text{out}} - T_{j,n}^{\text{in}})] \quad (14)$$

$$A_n = \Phi_n / (\Delta_{\ln} T_n U_n) \quad n \in \mathbf{N} \quad (15)$$

$$A_n^{\text{add}} \geq A_n - \sum_{n \in \mathbf{N}} A_{n,\text{ex}} \quad n \in \mathbf{N} \quad (16)$$

Equation 13 denotes the heat flow rate of the n^{th} heat exchanger (the same is true for the equations of new heat exchanger m ; $m = \text{HEST and HEW1}$). Equation 14 calculates the logarithmic-mean temperature difference. Equation 15 represents the area of the n^{th} heat exchanger. Equation 16 selects any additional area of the n^{th} heat exchanger.

A_n is the calculated additional area of an existing heat exchanger, it can be enlarged, or be left unchanged with an additional heat exchanger built in.

Additional equations for the mass balance of the u^{th} separation ($u = \text{F1, F2, F107, F108, and SEP}$; $u = 1, \dots, \mathbf{U}$), for all the components ($s = 1, \dots, \mathbf{S}$) are:

$$F_u^{\text{in}} = F_u^{\text{out,v}} + F_u^{\text{out,l}} \quad u = 1, \dots, \mathbf{U} \quad (17)$$

$$F_u^{\text{in}} \cdot x_{u,s}^{\text{in}} = F_u^{\text{out,v}} \cdot x_{u,s}^{\text{out,v}} + F_u^{\text{out,l}} \cdot x_{u,s}^{\text{out,l}} \quad u = 1, \dots, \mathbf{U} \quad s = 1, \dots, \mathbf{S} \quad (18)$$

$$\sum_s x_{u,s}^{\text{out,v}} = 1 \quad u = 1, \dots, \mathbf{U} \quad (19)$$

$$\sum_s x_{u,s}^{\text{out,l}} = 1 \quad u = 1, \dots, \mathbf{U} \quad (20)$$

$$K_{u,s} = d_{u,s} + c_{u,s} \cdot T_{i,n}^{\text{out}} + b_{u,s} \cdot (T_{i,n}^{\text{out}})^2 \quad u = 1, \dots, \mathbf{U} \quad s = 1, \dots, \mathbf{S} \quad (21)$$

where d_u , c_u , b_u are equilibrium constants in separation and x is amount fraction.

$$x_{u,s}^{\text{out,v}} = K_{u,s} \cdot x_{u,s}^{\text{out,l}} \quad u = 1, \dots, \mathbf{U} \quad s = 1, \dots, \mathbf{S} \quad (22)$$

The inlet amount flow rate for the u^{th} separation is the sum of the outlet's amount flow rates of the vapour and liquid phases (Eq. 17). Equation 18 includes the amount flow fractions for the components. The equilibrium constant of the s^{th}

component in the u^{th} separation is a function of temperature. The compositions of streams, using the separation model, are in relatively good agreement with experimental data within the existing methanol plant.

The temperatures at the outlets of polytropic compressors CP_c ($T_{\text{CP}_c}^{\text{out}}$; $c = \text{G201I, G201II, COMP1 and COMP2}$) depend on the inlet temperatures ($T_{\text{CP}_c}^{\text{in}}$), and can be calculated by equation 23:

$$T_{\text{CP}_c}^{\text{out}} = a_{\text{CP}_c} + b_{\text{CP}_c} \cdot T_{\text{CP}_c}^{\text{in}} \quad c = \text{G201I, G201II, COMP1, and COMP2} \quad (23)$$

where a_{CP} , b_{CP} are temperature constants for polytropic compression.

A linear relationship between the inlet and outlet temperatures can be used for small temperature

difference ($\Delta T = 20 \text{ K}$ for gases; real constraint). Using the linear model, the temperatures of streams are in relatively good agreement with measured data within the existing methanol plant.

The medium pressure of the turbine can be varied during the design. The turbine power (P_{tur}) is a function of the outlet temperature ($T_{\text{tur, out}}$), molar heat capacity (C_m), and the amount flow rate (F ; Eq. 24). The inlet temperature ($T_{\text{tur, in}}$) is constant:

$$P_{\text{tur}} = C_m \cdot (T_{\text{tur, in}} - T_{\text{tur, out}}) \cdot F \cdot \eta_{\text{tur}} \cdot \eta_{\text{gen}} \quad (24)$$

The thermodynamic efficiency of the medium pressure turbine (η_{tur}) and mechanical efficiency of the generator (η_{gen}) are supposed to be 85 % each [9].

The degrees of conversion after each catalyst bed-level can be predicted by mathematical methods [10]. The amount ratio between catalyst bed-levels $b - 1$ and b (from the set $b \in B$), $f_{s, b-1, b}$ can be calculated, if the amount fractions x_s of key components s (from the set $s \in S$) are known from experimental data:

$$f_{s, b-1, b} = x_{s, b-1} / x_{s, b} \quad s \in S \quad b \in B \quad (25)$$

The amount flow rate for component s at level b ($F_{s, b}$) can be estimated by dividing the amount flow rate at level $b - 1$ ($F_{s, b-1}$), and the ratio of the amount fraction ($f_{s, b-1, b}$):

$$F_{s, b} = F_{s, b-1} / f_{s, b-1, b} \quad s \in S \quad b \in B \quad (26)$$

The amount flow rate change for component s , reacting at level b ($\Delta F_{s, b}$), is given by the equation 27:

$$\Delta F_{s, b} = F_{s, b-1} - F_{s, b} \quad s \in S \quad b \in B \quad (27)$$

Finally, the degree of conversion (X_b) at level b can be calculated:

$$X_b = \Delta F_{s, b} / F_{s, b-1} \quad s \in S \quad b \in B \quad (28)$$

The degree of conversion can affect the composition of outlet gas from the reactor. The amount flow rate for component s at the last level B ($F_{s, B}$) can be estimated from the outlet gas composition of the reactor (F_B ; Eqs. 29-30), whether we have all the necessary existing data or not (equations 10-12 can be used). The compositions in the synthesis gas reactor REA-1 calculated by equations 29-30 are more exact:

$$F_{s, B} = F_{s, B-1} / f_{s, B-1, B} \quad s \in S \quad (29)$$

$$F_B = \sum_s F_{s, B} \quad (30)$$

The mechanism of catalytic process is not described here. The amount ratio between catalyst bed-levels and the degree of conversion after the catalyst-bed can be estimated by using simple mathematical equations (25-28), providing the amount fractions of the key components are known. The estimated degrees of conversion at the catalyst bed-level outlets give us some useful information about the degree of synthesis gas conversion, as the methanol production depends on the operating conditions of the reactor.

The NLP model includes only one type of fuel cell, a solid polymer membrane-type with molar energy, $E_{\text{fc}} = 100 \text{ kJ mol}^{-1}$. This fuel cell model was optimized parametrically by using the NLP algorithm with equations 2 and 3.

The mass balance of the PSA column in the NLP model is simplified with equations 5 and 6. Pressure swing adsorption uses an adsorber, packed with a molecular sieve, the adsorbent having efficiency over 50 % (existing industrial data). The PSA column is operated at a pressure of 26 bar, and temperature of 35 °C. The flow rate of hydrogen can be varied to within 0-488 kg/h. After start-up, the PSA column produces pure H_2 in 2-4 h. The purification system is completely automatic. H_2 purification cost in the existing PSA column and the inlet injection cost of recycling are 0.1 EUR/kg (industrial data). Pure H_2 can be used as fuel in the fuel cells.

The mathematical model of the process was applied, including the heat exchange of heat flows, generation of electricity in the generator connected to the gas turbine and in the fuel-cells, and increased production. The model contained equations for parameter optimisation, together with process operating constraints. The objective function (Eq. 31) of the NLP model maximized the annual profit V_{max} ; it included electricity cogeneration in a gas turbine ($P_{\text{tur}} \eta_{\text{tur}} \eta_{\text{gen}}$) and fuel-cells (P_{fc}), heat flow rate in fuel-cells (Φ_{fc}), increased methanol production (ΔF_M), and decreased raw material mass flow rate of the high pressure steam, ΔF_{steam} , from 33.1 t/h to 32 t/h in the reactor REA-1 (Table 1). The variable parameters in the objective function are shown bold.

$$\begin{aligned}
V_{\max} = & C_{\text{el}} \cdot P_{\text{tur}} \cdot \eta_{\text{tur}} \cdot \eta_{\text{gen}} + C_{\text{el}} \cdot P_{\text{fc}} + C_{\text{heat}} \cdot \Phi_{\text{fc}} + C_{\text{M}} \cdot \Delta F_{\text{M}} + C_{37} \cdot \Delta F_{\text{steam}} \\
& - C_{37} \cdot \Phi_{\text{HEST}} - (22\,946 + 13.5 \cdot P_{\text{tur}}) \cdot 4 - [2\,605 \cdot P_{\text{COMP1}}^{0.82} - 2\,605 \cdot P_{\text{COMP2}}^{0.82} \\
& - \sum_{\text{add}} (8600 + 670 \cdot A_{\text{HE, new}}^{0.83}) \cdot 7 - \sum_{\text{new}} 670 \cdot \Delta A_{\text{HE, add}}^{0.83} \cdot 3.5 \cdot 2] \cdot r \\
& - C_{\text{H}_2} \cdot F_{\text{H}_2} \cdot r - C_{\text{fc}} \cdot P_{\text{fc}} \cdot r
\end{aligned} \tag{31}$$

new = HEST, HEW1; add = HEW, HEA, HEPR

The inlet stream of reactor REA-2 can be heated by a process stream in the heat exchanger (HEPR) and/or by high pressure steam (HEST) using varying heat flow rates. The available heat from cooling the synthesis gas (heat exchangers E107-E112) is used for 37 bar steam production, the process including more process-utility than process-process heat flow exchange. In this model, the existing areas can be used ($A_{\text{HE, ex}}$), by enlarging them with additional areas ($\Delta A_{\text{HE, add}}$), if necessary. All process units are not operated at maximal capacity. Additional annual depreciation of the enlarged and new areas ($A_{\text{HE, new}}$) of the heat exchangers and compressors (Table 1) is multiplied by the payback multiplier ($r = 0.216$, which

includes the 8 % rate of interest and 10 years lifetime without another factors; [11]), and corrected for inflation. Operability and control issues have not been dealt with so far.

3.3. Suggested retrofit

The retrofitted methanol process (Fig. 4) was selected with electricity generation using the gas turbine, the pressure of which should be dropped from 49.7 bar to 37 bar, and outlet temperature, $T_{\text{tur, out}} = 110 \text{ }^\circ\text{C}$.

The existing PSA column could be used for purifying a maximum 488 kg/h of H_2 supplied as fuel to fuel cells, which could produce 6.75 MW

Table 1. Cost items for the example process.

Installed cost of heat exchanger*/EUR: $(8\,600 + 670 A^{0.83}) \cdot 7^\#$
Depreciation of compressor, $C_{\text{com}}^\&/\text{EUR}$: $2\,605 \cdot P^{0.82}$
Depreciation of gas turbine, $C_{\text{tur}}^\&/(\text{EUR/a})$: $(22\,946 + 13.5 P_{\text{tur}}) \cdot 4^\#$
Price of methanol, $C_{\text{M}}^+/\text{(EUR/t)}$: 115
Price of heat, $C_{\text{heat}}^{**}/(\text{EUR/kW} \cdot \text{a})$: 60
Cost and taxes of CO_2 emissions, $C_{\text{tax}}^{++}/(\text{EUR/t})$: 22
Cost of electricity, $C_{\text{el}}^{**}/(\text{EUR}/(\text{kW} \cdot \text{a}))$: 435.4
Cost of fuel-cells, $C_{\text{fc}}^{***}/(\text{EUR/kW})$: 2 125
Cost of H_2 purification in existing PSA column and inlet injection in recycle, $C_{\text{H}_2}/(\text{EUR/kg})$: 0.1
Cost of 37 bar steam (P_{37}) ^{**} /($\text{EUR}/(\text{kW} \cdot \text{a})$): 106.3

*** [6]

* [12]; A = area in m^2

** [13]

& [4]; P = power in kW

++ Axelsson *et al.*, 2003

+ ten years average

the published cost equations for the equipment are adjusted to the real, higher industrial costs, by the multiplier of 2.

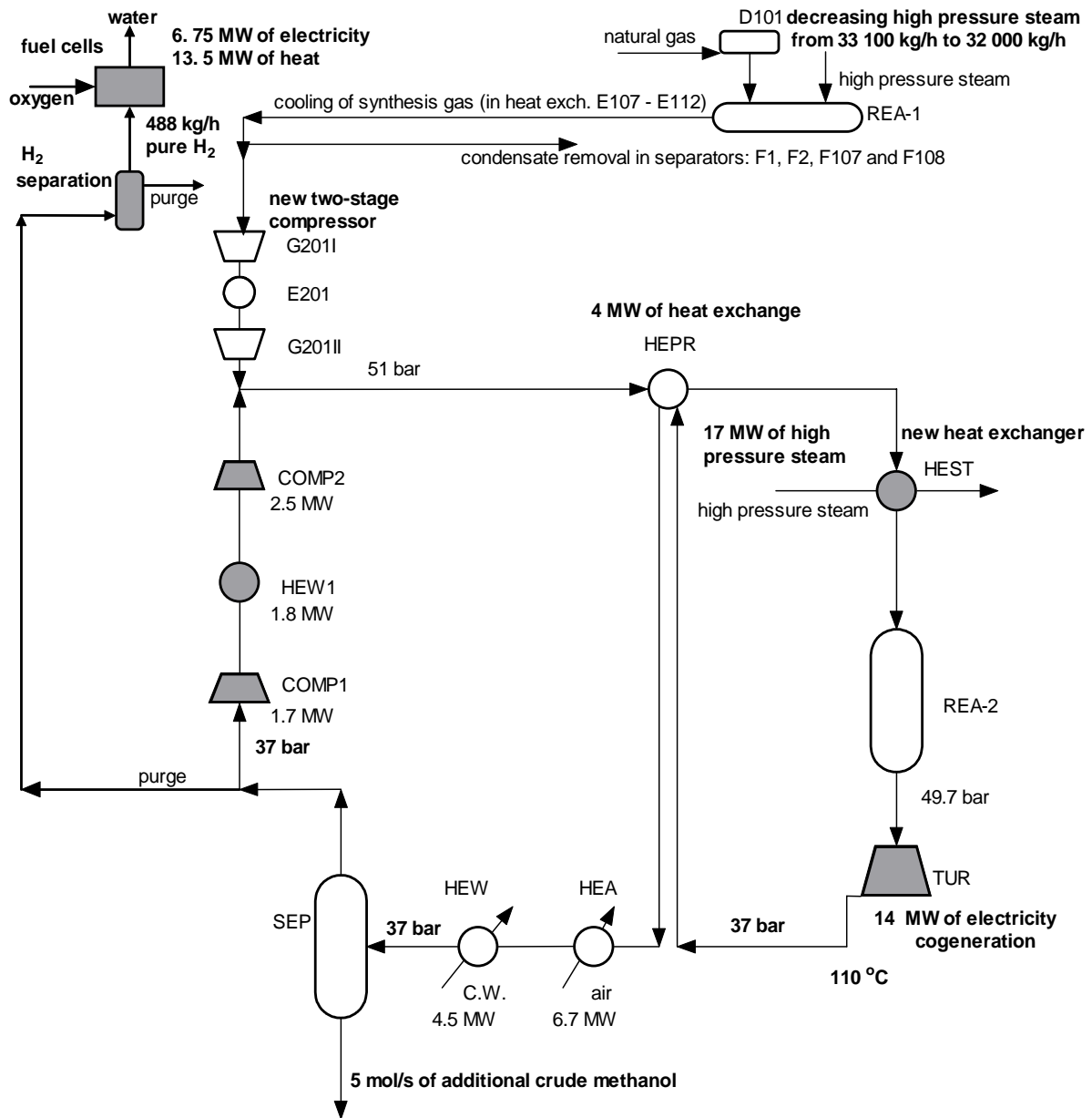


Figure 4. Simplified flow sheet of the retrofitted methanol plant.

of electricity and 13.5 MW of heat. The total additional annual methanol production is estimated to be 5 mol/s. This structure enables 14 MW of electric power to be generated in the gas turbine. The steam exchanger (HEST) needs 17 MW of heat flow rate. The integrated process stream exchanges 4 MW of heat flow rate in HEPR. The powers of the first and second compressor stages are 1.7 MW and 2.5 MW, respectively. The HEW1 is supposed to exchange

1.8 MW, the coolers HEW and HEA 4.5 MW and 6.7 MW of heat flow rate, respectively. The purge gas outlet flow rate fraction should be decreased from 5.9 % to 5.4 %. The existing coolers of the synthesis gas (E107, E109, E110, E111, E112 and E201) need not be enlarged for optimal 37 bar steam production [7]. The additional annual depreciation of the gas turbine, the new heat exchangers (HEST, HEW1, having 942 m² and 324 m² of area, respectively), and the

Table 2. Retrofit economics.

Annual depreciation of:	
• Gas turbine:	1.07 MEUR/a
• New heat exchangers:	0.44 MEUR/a
• New two stages compressor:	0.59 MEUR/a
• Fuel cell:	3.00 MEUR/a
The cost of high pressure steam:	1.80 MEUR/a
The cost of hydrogen purification:	0.40 MEUR/a
Contingency:	0.35 MEUR/a
Annual income of:	
• Electricity in gas turbine:	6.00 MEUR/a
• Additional methanol production:	0.50 MEUR/a
• Steam saving:	0.06 MEUR/a
• Electricity in fuel cells:	2.94 MEUR/a
• Available heat in fuel cells:	0.80 MEUR/a
Total additional profit of retrofit:	2.65 MEUR/a

new two stage compressor is estimated to be 2.1 MEUR/a ($1.07 + 0.44 + 0.59 = 2.1$ MEUR/a). Table 2 presents other elements of the retrofit economics. The economics of the retrofit is presented in Table 2. The NLP program includes 135 equations and 140 variables with a computation time of 17.5 s, using VAX-3100, and the GAMS program.

The economical analysis shows that electricity cogeneration in the gas turbine is very economical and profitable, with a payback time of $t_{PB} \approx 2.2$ a, but electricity generation in fuel cells is less profitable because of higher annual depreciation of fuel cells, having a payback time of $t_{PB} \approx 4.2$ a.

CONCLUSIONS

Different mathematical methods can be used for process optimization, but for nontrivial and complex retrofit, with many real operational constraints (capacity, temperature and pressure) the NLP is very useful [7]. This procedure does not guarantee a global cost optimum, but it does lead to good retrofit, perhaps near-optimum one.

Multi-parameter energy and process systems' optimization is an activity which can yield good ideas for chemical plant process design or retrofit. This paper presents an efficient use of NLP model

formulation for the simultaneous cogeneration of electricity and steam using a gas turbine, as well as maximum heat exchange. The hydrogen can be separated from purge gas by using an adsorption system, to be then used as fuel in the fuel-cells. Low temperature fuel-cells can operate efficiently by using pure hydrogen. Continuous hydrogen separation and energy generation in fuel cells needs no storage of hydrogen.

An important characteristic of a catalyst is its effect on selectivity. The amount ratios between catalyst bed-levels and the degrees of conversion after the catalyst bed-levels can be estimated by using simple mathematical equations, if the amount fractions of the key components are known. The estimated degrees of conversion at the catalyst bed-level outlets give useful information about the degree of synthesis gas conversion.

The NLP model was formulated using a simplified process structure and was found to be a very effective tool for the optimization of complex process retrofits. This simultaneous mathematical optimisation method gives a near optimum solution, probably close to a global one. We have carried-out simultaneous heat flow, power and product optimization in a methanol plant with an additional potential profit of 2.65 MEUR/a.

NOMENCLATURE**Abbreviations:**

CHP	= combined heat and power
COMP	= compressor
HE	= heat exchanger
MINLP	= mixed integer nonlinear programming
NLP	= nonlinear programming
PSA	= pressure swing adsorption
SPM	= solid polymer membrane-type fuel cells

Indices:

<i>b</i>	= catalyst bed-level
<i>c</i>	= compressor
<i>fc</i>	= fuel cell
<i>i</i>	= hot process or utility stream
<i>j</i>	= cold process or utility stream
<i>l</i>	= liquid phase
<i>m</i>	= new heat exchanger
<i>n</i>	= existing heat exchanger
<i>r</i>	= reaction
<i>s</i>	= component
<i>u</i>	= separator
<i>v</i>	= vapour phase

Sets:

B	= { <i>b</i> <i>b</i> is a catalyst bed-level}
N	= { <i>n</i> <i>n</i> is an existing heat exchanger}
R	= { <i>r</i> <i>r</i> is a reaction}
S	= { <i>s</i> <i>s</i> is a component}

Parameters:

a_{CP}	= temperature constant for polytropic compression
$A_{n,ex}$	= area of an existing heat exchanger, m ²
a_r	= heat capacity constants of reaction <i>r</i>
b_{CP}	= temperature constant for polytropic compression
b_u	= equilibrium constant in separation <i>u</i>
b_r	= heat capacity constants of reaction <i>r</i>
c_r	= heat capacity constant of reaction <i>r</i>
c_u	= equilibrium constant in separation <i>u</i>
d_r	= heat capacity constant of reaction <i>r</i>
d_u	= equilibrium constant in separation <i>u</i>
E	= molar energy, kJ mol ⁻¹
I_r	= integration constant of reaction <i>r</i>
J_r	= integration constant of reaction <i>r</i>

$K_{u,s}$	= equilibrium constant of component <i>s</i> in separation <i>u</i>
r	= pay back multiplier
U	= overall heat transfer coefficient, W/(m ² K)
y	= equilibrium gas composition

Variables:

A_n^{add}	= additional area of heat exchanger <i>n</i> , m ²
A_n	= total area of existing heat exchanger <i>n</i> , m ²
C	= cost, EUR
C_m	= molar heat capacity, J/(mol K)
$CF_{i,n}$	= heat capacity flow rate of hot stream <i>i</i> in HE <i>n</i> , W/K
G	= Gibbs energy, J
F	= amount flow rate, mol/s
f	= ratio of amount fraction
K_r	= equilibrium constant of reaction <i>r</i>
n	= amount, mol
p	= pressure, bar
P	= power, W
P	= price, EUR
T	= temperature, K
V_{max}	= maximum additional annual profit, EUR/a
x	= amount fraction, 1
X	= degree of conversion, 1
y	= equilibrium gas composition
ν	= stoichiometric coefficient
η	= efficiency, 1
Φ	= heat flow rate, W
$\Delta_{ln}T_n$	= log-mean temperature difference of heat exchanger <i>n</i> th , K
ξ	= extent of reaction, mol
ω_r	= equilibrium conversion, mol/s

REFERENCES

1. Horlock, J. H. 1987, Pergamon Press, Oxford.
2. Havelky, V. 1999, International Journal of Refrigeration, 22, 479-485.
3. Axelsson, H., Harvey, S., Asblad, A., and Berntsson, T. 2003, Applied Thermal Engng., 23, 65-87.
4. Biegler, L. T., Grossmann, I. E., and Westerberg, A. W. 1997, Prentice Hall, Upper Saddle River, New Jersey, 1-408.

-
5. Skrzypek, J., Lachowska, M., and Serafin, D. 1990, *Chemical Engineering Science*, 45, 1, 89-96.
 6. Shin'ya, O. 2006, *Renewable Energy*, 32, 3, 382-406.
 7. Kovač Kralj, A., Glavič, P., and Kravanja, Z. 2000, *Comput. Chem. Engng.*, 24, 1, 125-138.
 8. Brooke, A., Kendrick, D., and Meeraus, A. 1992, Palo Alto, Scientific Press.
 9. Kraut, B. 1994, Technical publishing Slovenia, Ljubljana, 245.
 10. Kovač Kralj, A. and Glavič, P. 2007, *J. Ind. Eng. Chem. - Korean Soc. Ind. Eng. Chem.*, 13, 5, 723-728.
 11. Ahmad, S. 1985, Institute of Science and Technology, Manchester, 113 and 306.
 12. Tjoe, T. N. and Linnhoff, B. 1986, *Chem. Engng.*, 28, 47-60.
 13. Swaney, R. 1989, *AIChE Journal*, 35, 6, 1010.